

This is an Accepted Manuscript of the following article:

D T Myat, F Roddik, P Puspita, L Skillman, J Charrois, I Kristiana, W Uhl, E Vasyukova, G Roeszler, A Chan, B Zhu, S Muthukumaran, S Gray, M Duke. Effect of oxidation with coagulation and ceramic microfiltration pre-treatment on reverse osmosis for desalination of recycled wastewater. *Desalination*. Volume 431, 2018, pages 106-118, ISSN 0011-9164.

The article has been published in final form by Elsevier at

<http://dx.doi.org/10.1016/j.desal.2017.10.029>

© 2018. This manuscript version is made available under the

CC-BY-NC-ND 4.0 license

<http://creativecommons.org/licenses/by-nc-nd/4.0/>

It is recommended to use the published version for citation.

1 Effect of oxidation with coagulation and ceramic microfiltration pre-
2 treatment on reverse osmosis for desalination of recycled wastewater

3 **D. T. Myat¹, F. Roddick², P. Puspita², L. Skillman³, J. Charrois⁴, I. Kristiana⁴, W.**
4 **Uhl^{5,6}, E. Vasyukova^{5,7}, G. Roeszler⁸, A. Chan⁹, B. Zhu¹, S. Muthukumaran¹, S. Gray¹,**
5 **M. Duke¹**

6 *¹Institute for Sustainability and Innovation, College of Engineering and Science, Victoria*
7 *University, Werribee Campus, P. O. Box 14428, Melbourne, Vic 8001, Australia.*

8 *²Water: Effective Technologies and Tools (WETT) Research Centre, RMIT University,*
9 *G.P.O. Box 2476V, Melbourne, 3001, Australia*

10 *³School of Engineering and Information Technology, Murdoch University, South Street,*
11 *Murdoch. WA 6150, Australia*

12 *⁴Curtin Water Quality Research Centre, Department of Chemistry, Curtin University, Perth,*
13 *WA 6102, Australia*

14 *⁵Technische Universität Dresden, Chair of Water Supply Engineering, 01069 Dresden,*
15 *Germany*

16 *⁶Norwegian Institute for Water Research (NIVA), Gaustadalléen 21, 0349 Oslo, Norway*

17 *⁷WTE Wassertechnik GmbH, Ruhrallee 185, 45136 Essen, Germany*

18 *⁸Water Research Australia (WaterRA), G.P.O. Box 1751 Adelaide 5001, Australia*

19 *⁹City West Water, 1 McNab Ave, Footscray, Victoria, 3011, Australia*

20
21 *Corresponding author: Mikel Duke. Email: Mikel.Duke@vu.edu.au*

22 **Abstract**

23 Oxidation and coagulation before ceramic microfiltration (CMF) greatly increases membrane
24 flux, but is unconventional for reverse osmosis (RO) pre-treatment. Impacts to RO and the
25 wastewater recycling scheme operating CMF at high flux conditions is little understood. In
26 this work, wastewater was treated with ozone or ultraviolet/hydrogen peroxide (UVH)
27 oxidation, coagulation, then CMF, to explore RO membrane performance at bench scale.
28 Sustainable high CMF fluxes were confirmed using coagulation with either ozone or UVH.
29 Uniquely for ozone, dosing 13 mg-O₃/L for 15 minutes greatly increased toxic by-product N-
30 nitrosodimethylamine (NDMA) to 33 ng/L. Dosing chloramine (common for RO biofouling
31 control) added only up to 7 ng/L NDMA. RO tests on all pre-treated waters showed little
32 variation to flux but oxidation significantly altered texture of RO fouling material from
33 smooth and dense to porous and granular. Biofouling studies with model bacteria strain RO
34 22 (*Pseudoalteromonas* spp) showed higher organic biodegradability but biofilm analysis

35 revealed ozone-coagulant-CMF greatly limited extension of bacteria communities from the
36 membrane surface suggesting oxidation reduces RO biofouling. The novel findings of
37 reduction of RO biofouling risk with oxidation and coagulation for high flux CMF pre-
38 treatment identified in this work need to be demonstrated on different wastewater types over
39 longer term.

40 Keywords: Biofouling, ceramic membrane, coagulation, oxidation, ozone, pre-treatment,
41 recycled water, reverse osmosis, ultraviolet /hydrogen peroxide (UVH)

42

43 **Introduction**

44 Ceramic membranes are an alternative technology to polymeric membranes for water treatment
45 offering superior physical integrity, chemical resistance, higher flux, and longer life [1].
46 However their application as a pre-treatment for reverse osmosis (RO) desalination of
47 wastewater is unconventional. In considering ceramic membranes, high flux is important to
48 offset their higher material cost but must be operated in a specific way to achieve this, which
49 would impact the downstream RO plant operation. For example Dow and co-workers
50 demonstrated that the sustainable ceramic microfiltration (CMF) membrane fluxes for treating
51 clarified wastewater increased 2-3 fold in response to dosing with the common coagulant
52 polyaluminium chloride (PACl) [2, 3]. Coagulation used prior to polymer membranes is
53 already known to reduce fouling as well as to remove organic matter, particularly the large
54 molecular weight (MW) components, being biopolymers and humic substances [4-6]. Fan et
55 al. [7] concluded that coagulation treatment reduced organic fouling by removal of these larger-
56 sized materials. Further, ozone used in conjunction with coagulation and ceramic membranes
57 was observed to work together to provide >4-fold sustainable flux increases for ceramic
58 membranes [2]. Oxidation processes such as ozonation, and ultraviolet irradiation (UV), are
59 commonly practised as the tertiary treatments to meet appropriate water quality in reclaimed
60 water from secondary wastewater treatment plant (WWTP) effluents for disinfection purposes,
61 odour treatment as well as the removal of colour caused by humic substances. With their wider
62 use in water treatment, researchers have more recently considered their specific impact on
63 water organic fractions [6, 8] and membrane fouling [9], which is particularly useful for
64 explaining why such high ceramic membrane fluxes can be achieved.

65

66 Studies conducted using ozone-resistant polyvinylidene fluoride (PVDF) and polysulfone (PS)
67 membrane materials showed that using ozonation upstream of the membrane did enhance the
68 permeate flux and reduce membrane fouling by the degradation of high molecular weight
69 natural organic matter [10-13]. More recently, a study on polymer ultrafiltration (UF)
70 membranes found that the mechanisms are more complex, where ozone reactions with bovine
71 serum albumin (BSA) led to increased fouling, while reactions with alginate led to reduced
72 fouling [9]. On top of altered organics chemistry, theories around the role of ozone regarding
73 its ability to greatly enhance flux have focused on the role of highly reactive hydroxyl radicals
74 (OH^\bullet) formed by the catalytic breakdown of ozone on the ceramic membrane surface [14].

75

76 So in the case of upstream oxidation where membranes benefit in terms of performance, there
77 is a clear alteration of the chemical properties of the water borne compounds that will impact
78 other downstream processes. In the case of saline wastewater, low pressure membranes are
79 widely applied prior to reverse osmosis (RO) as a pre-treatment. Normally oxidation would be
80 applied in a water recycling scheme downstream of RO, however, it is generally understood
81 that the mechanisms to increase hydrophilicity of organics in wastewater would be useful in
82 controlling RO membrane fouling. Such benefits including minimising cleaning and membrane
83 replacement, and reduced energy requirements due to reduced RO fouling, were explored in a
84 dedicated study [15]. Membrane bioreactor (MBR) effluent was fed directly to a dual train pilot
85 RO system with one train featuring an ozone stage, while the other fed directly by MBR
86 permeate. The reduction to membrane fouling was demonstrated over 3000 hours of testing,
87 showing reduced membrane permeability deterioration suggesting longer term benefits to RO
88 membranes in terms of longevity, reduced cleaning costs and lower energy requirement [15].
89 Without ozone, RO flux declined by 12% while with ozone only declined by 6%. Similar
90 beneficial effects were reported at bench scale [16]. Recent work on application of ozone and
91 CMF followed by biologically active filtration upstream of RO for water recycling application
92 found uniquely that RO foulants after ozone and CMF were easily removed with water rinsing
93 [17]. This promising finding shows that in the case when ozone is applied upstream, reduced
94 cleaning maintenance of the RO membranes is expected. The process was subsequently
95 adopted for a 9 month potable reuse trial [18, 19]. However, these used biological processes
96 after oxidation, may not be necessary to apply prior to RO.

97
98 Oxidation (i.e., ozone or UV) in practice is typically followed by biological filtration. Ozone
99 breaks down larger molecular weight organic matter increasing the assimilable organic carbon
100 proportion, favouring micro-organism growth [20]. The study by Nguyen and Roddick
101 highlighted that the ozonation of the raw activated sludge effluent produced biodegradable
102 dissolved organic carbon (BDOC), and biological activated carbon (BAC) filter did not
103 completely remove those compounds [21]. Thus it is uncertain if deliberate use of BAC to
104 prevent biofouling of downstream RO membranes would be effective. Recent work has shown
105 that ozone and BAC application prior to ceramic membranes can have a negative impact to
106 CMF performance compared to ozone on its own [22] suggesting that despite the BDOC
107 removing ability of BAC, it is not useful for high CMF performance and could be avoided for
108 pre-treatment to RO.

109
110 Disinfection by chloramines is generally practised prior to the RO process to prevent the
111 membrane from biofouling in a conventional RO-based water recycling application [23].
112 Hence, despite the increase in biodegradability of organics due to ozone, the application of
113 chloramine may assist in controlling biofouling. However, the use of chloramines can lead to
114 the formation of disinfection by-products (DBPs), especially nitrogen-containing DBPs such
115 as *N*-nitrosodimethylamine (NDMA) and other *N*-nitrosamine compounds [24]. On top of this,
116 ozone is also well-known to form NDMA as a result of the oxidation of NDMA precursors [25-
117 28]. NDMA is an important concern if the intended use of the water is limited by this
118 compound, e.g., potable reuse. A study on ozone application upstream of RO should consider
119 use of chloramine disinfectant and the formation of NDMA.

120

121 Therefore, it still remains unknown of the viability of using the high CMF flux arrangement
122 (with oxidation and coagulation) as a pre-treatment to RO for saline wastewater recycling
123 purpose, particularly in the case where no post-oxidation biological treatment stage (e.g. BAC)
124 is used. At the same time, working towards understanding differences in RO membrane fouling
125 (both organic and bio) of this non-traditional water recycling process compared to the more
126 traditional approach (without oxidation prior to RO) is of more fundamental interest.
127 Addressing these points forms the more novel feature of this work. This study therefore has the
128 following objectives 1) to confirm reported high flux performance when ceramic membranes
129 are coupled with coagulation, ozonation and UV/H₂O₂ (UVH) treatment and their
130 combinations; 2) to demonstrate the impact of the pre-treatment processes on water quality
131 including formation of a well-known wastewater disinfection by-product, NDMA; 3) to test
132 the influence of the pre-treatment options on RO membrane performance; and 4) to determine
133 the potential for biofouling on the downstream RO membranes. The source water collected
134 from a full-scale water recycling plant was used for the purpose of this work.

135

136 **Materials and Methods**

137 *Raw water source*

138 The water source used for this study was ‘Class A’ recycled water from one of Melbourne’s
139 wastewater treatment plants (WWTP) run by the authorised operator. The WWTP receives
140 wastewater from both domestic and industrial sources. To meet Class A specification, the
141 incoming sewage is treated via an anaerobic and aerobic process followed by chlorination and
142 UV treatment. The recycled Class A water has characteristics as indicated in Table 1, measured
143 by methods described later under the ‘Water quality analyses’ section. This water is referred to
144 as ‘direct Class A’ water hereinafter. This water is currently fed to a recently constructed salt
145 reduction plant (SRP) which consists of a polymeric UF/RO system for water recycling
146 application and is therefore a good model water to show an alternative ozone and CMF as a
147 RO pre-treatment.

148

149 **Table 1:** Representative water quality indicators of Class A recycled wastewater used for this
150 work. Method for determination described under ‘Water quality analyses’ section.

Indicator	Unit	Value
pH	-	7.7
EC	µS/cm	1700
TDS	mg/L	1240
UV ₂₅₄	l/m	17.9
DOC	mg-C/L	10.5
COD	mg/L	38
TN	mg/L	15.8

151 EC = electrical conductivity, TDS = total dissolved solids, COD = chemical oxygen demand,

152 TN = total nitrogen

153

154 *Pre-treatments*

155 Pre-treatments to CMF included coagulation which was used in conjunction with ozonation or
156 UVH. For coagulation treatment with polyaluminium chloride (PACl), 23% w/w as (Al₂O₃)
157 from Ixom Watercare Pty Ltd, was dosed at 3 mg (Al³⁺)/L. This dose was chosen following a
158 series of jar tests where pin-floc was observed to start (visual observation of small flocs in
159 solution). The required amount of PACl coagulant was added to the feed tank prior to CMF
160 membrane, (and after oxidation by ozone or UVH when applied) without filtering the solids,
161 to simulate the inline coagulation process used in pilot trials [2]. Ozone was generated from
162 pure oxygen by an ozone generator (SOZ-6G, A2Z Ozone Systems Inc., USA) with an ozone
163 production capacity of 6 g/h. Further details of the ozone dosing and analysis is provided in the
164 Supplementary Material. During the ozone–CMF experiments, the feed water sample was
165 ozonated for 15 minutes which was determined to be equivalent to an applied dose of 13 mg-
166 O₃/L. Residual ozone present in the ozonated samples was not quenched, and it was allowed to
167 be in contact with the ceramic membrane surface. Ozone concentration was measured using
168 the Indigo Colorimetric method [29]. For UVH treatment, irradiation was conducted in an
169 annular reactor fitted with a centrally mounted UV lamp. It had a working volume of 900 mL
170 and an average irradiated area of 464 cm², with a path length of 1.95 cm. The UVC lamp
171 emitted monochromatic light at 254 nm. The average fluence rate of the UVC lamp was
172 determined to be 13.1 mW/cm² by hydrogen peroxide actinometry [30]. The effluent samples
173 were irradiated for various times with the addition of hydrogen peroxide (1 mM). This
174 treatment is referred to as UVH hereafter.

175

176 *Ceramic microfiltration (CMF)*

177 A Membralox T1-70 single channel ceramic membrane (Pall Corporation), which had a
178 separation layer of 0.1 µm nominal pore size, was used for CMF. The ceramic membrane had
179 dimensions of 250 mm length and 77 mm internal diameter, a total surface area of 0.005 m²,
180 and was composed of a porous alumina support and selective layer made from zirconia. An
181 example clean water flux measured for this membrane was 90 L/(m².h) at 0.1 bar. Further
182 details on the module, performance checking and cleaning are found in the Supplementary
183 Material. The ceramic membrane was tested in dead-end, constant flux, inside-out filtration
184 mode. Hydraulic backwashing was performed every 30 min at 3 bar via pressurised water and
185 a series of valves. A constant flux of 130 L/(m².h) was utilised for all CMF tests for the high
186 flux operation. More details of the equipment and the method for determining constant flux are
187 described in the Supplementary Material.

188

189 Filtration performance was evaluated by using indicators such as fouling rate and backwash
190 effectiveness (fouling reversibility). The rate of foulant accumulation on the membrane or
191 fouling rate over time was described as the change in transmembrane pressure (TMP) per unit

192 time ($dTMP/dt$) on a per cycle basis. The change in fouling rate (%) was calculated by the
 193 following equation [31]:

$$194 \quad \text{Change in fouling rate (\%)} = \frac{\left(\frac{dTMP}{dt}_n\right) - \left(\frac{dTMP}{dt}_1\right)}{\left(\frac{dTMP}{dt}_1\right)} 100 \quad (1)$$

195 where the fouling rate of the final filtration cycle (cycle n) was compared to the initial filtration
 196 cycle (cycle 1).

197 To assess membrane performance data between filtration and backwash cycles, the following
 198 method was used based on the unified membrane fouling index (UMFI) developed by Huang
 199 et al. (2008) [32] and Nguyen et al. (2011) [33]. All TMP data points were used to calculate
 200 specific flux or permeability, J_s , (L/(m².h.bar)) as follows:

$$201 \quad J_s = J/TMP = 1/\mu (K_{mem} + k_{total} V) \quad (2)$$

202 Where μ is viscosity, K_{mem} is the resistance of the clean membrane, k_{total} is the total resistance
 203 (membrane and fouling resistances), and V is the specific volume (L/m²).
 204

205 For a clean membrane, at $V = 0$, $(J/TMP)_0 = 1/\mu K_{mem}$. Membrane performance can be
 206 represented in normalized form, J'_s , by dividing J/TMP at any specific volume by the initial
 207 (or clean membrane) condition according to the following equation:
 208

$$209 \quad J'_s = \frac{\left(\frac{J}{TMP}\right)_V}{\left(\frac{J}{TMP}\right)_0} = \frac{1}{1 + \frac{k_{total}}{K_{mem}} V} \quad (3)$$

210
 211 or

$$212 \quad \frac{1}{J'_s} = 1 + \left(\frac{k_{total}}{K_{mem}}\right) V \quad (4)$$

213 Different fouling indices could be calculated from plotting a graph of $1/J'_s$ versus V . Hydraulic
 214 irreversible fouling index (HIFI) can be calculated using the starting TMP data point after each
 215 backwash cycle. HIFI is related to the fouling resistance and a low HIFI represents a low rate
 216 of membrane fouling while a high HIFI indicates greater membrane fouling rates.
 217

218 *RO feed chlorination, membrane fouling loading tests and SEM analysis*

219 A dose of preformed chloramine was added to each filtrate of the CMF as per the conditions
 220 established on current RO systems (approximately 4 mg/L) and similar to previous studies [16,
 221 34]. For antiscalant dosing, the commonly used Flocon 260 was dosed at 3 mg/L to the solution
 222 to represent realistic application to RO feeds.

227 The RO membrane fouling loading test for the pre-treated waters was performed on a DOW
228 FILMTEC BW-30 membrane. The schematic diagram of RO membrane filtration set up and
229 further details of the operation are found in the Supplementary Material. The effective
230 membrane area was 0.014 m² and cross flow velocity of 0.2-0.3 m s⁻¹, and run in batch
231 concentration to achieve a final volume recovery of 80%. Pressure of the feed was set to 10
232 bar.

233 SEM was employed to investigate the morphology of the membrane surface and accumulated
234 fouling material. The SEM images were produced using a NeoScope JCM5000 (JEOL, Japan)
235 with a 10 kV electron beam. To improve the imaging of the samples, the membranes were gold
236 coated using a Neo coater MP-19020NCTR (JEOL, Japan) prior to the observations.

237

238 *Water quality analyses*

239 The feed samples before and after pre-treatments were analysed for pH, electrical conductivity
240 (EC), ultraviolet absorbance at 254 nm (UV₂₅₄) and dissolved organic carbon (DOC). Some
241 indicators were measured and shown only in Table 1 to give an overview of the water quality
242 (i.e. includes also TDS, COD and TN). pH and EC were determined using a HACH Sension
243 156 handheld meter. TDS was determined using Standard Method 2504. UV₂₅₄ was measured
244 using an HACH DR 5000 spectrophotometer. Specific UV absorbance (SUVA) was
245 determined by dividing UV₂₅₄ by the DOC concentration. DOC and TN concentrations were
246 measured using a total organic carbon analyser (TOC-V_{CPH}/CPN, Shimadzu, Japan). DOC
247 fractionation was performed by liquid size exclusion chromatography with organic carbon
248 detection (LC-OCD) using a LC-OCD model 8 system (DOC-Labor Dr. Huber, Karlsruhe,
249 Germany) at Technische Universität Dresden, Germany. LC-OCD enables the characterisation
250 and quantification of DOC fractions. Details of the method have been published elsewhere [35,
251 36] and a further summary can be found in the Supplementary Material.

252 The concentration of biodegradable dissolved organic carbon (BDOC) of the waters before and
253 after treatments was determined using the method of Joret and Levi (1986) [37] and modified
254 according to the method reported by Volk et al., (1993) [38]. Briefly, a sample of 300 mL was
255 exposed to washed biologically active sand (100 ± 10 g) for 7 days under aerobic conditions (3
256 litres of humidified air per hour). The BDOC was calculated as the initial DOC minus the
257 lowest DOC recorded over the 7-day incubation period.

258 The chloraminated (4 mg/L as Cl₂) ceramic membrane permeate samples were analysed for N-
259 nitrosamines analysis after 4 mg/L chloramine dosing. N-nitrosamines were analysed by solid-
260 phase extraction (SPE) followed by gas chromatograph with mass spectrometer detector (GC-
261 MS), based on the method of Charrois et al. (2004) [39] with minor modifications. Further
262 details of the method are found in the Supplementary Material section.

263

264 *Bioassay and accelerated RO biofouling tests*

265 Biofilm assays were conducted using a crystal violet assay method [40]. A model biofouling
266 bacterial strain, RO 22, was used to evaluate the biofouling potential of the treated waters.

267 RO 22 is a strain of *Pseudoalteromonas* spp isolated from a full scale SWRO plant [41].
 268 Additional details of the organism and methods are found in the Supplementary Material. A
 269 single colony of isolate RO 22 was inoculated into 10 mL of tryptone soy broth (TSB) and
 270 mixed well. 200 μ L of culture broth was pipetted into each well in a 96-well microtitre plate,
 271 sealed and incubated for 48 hours at room temperature. Optical density of the wells to
 272 determine cell density, then removal of solution and addition of crystal violet to measure
 273 biofilm thickness, were both measured using light absorbance. For the accelerated biofouling
 274 tests, RO feeds where spiked with RO 22. The biofouling tests were conducted for a total of
 275 21 h. After 21 h of RO filtration tests, a dose of preformed chloramine (approximately 4
 276 mg/L) was added to the feed reservoir to observe effects due to the chloramine addition. At
 277 the end of each biofouling experiment, the membrane coupon was carefully removed and the
 278 membranes were preserved for confocal microscopic observation.

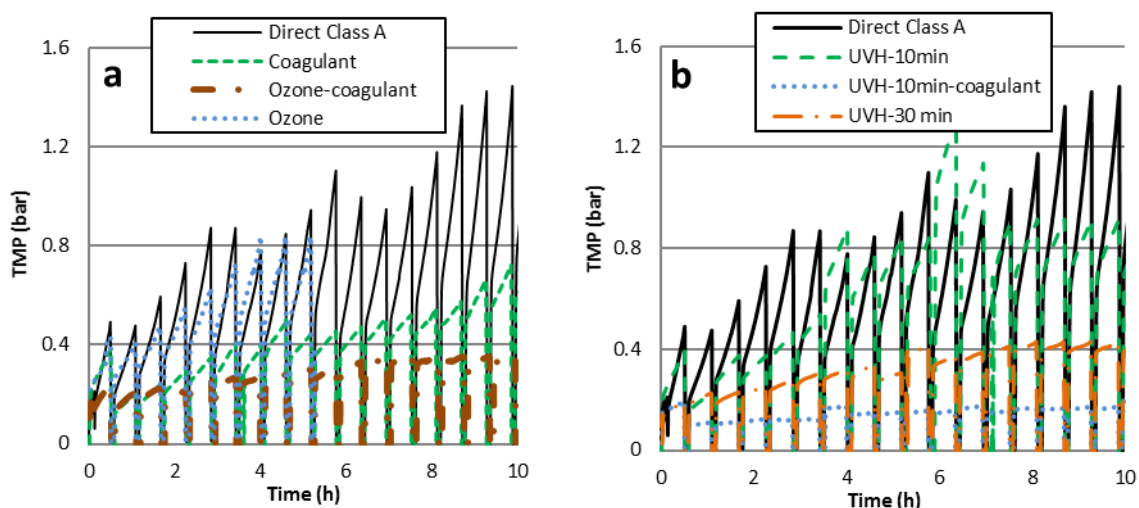
279

280 Results and Discussion

281 Ceramic membrane operation performance

282 Figure 1 shows the transmembrane pressure (TMP) profile of each process operated at
 283 constant CMF flux of 130 L/(m².h). Figure 1a shows TMP profiles during filtration of direct
 284 Class A water, and the same waters after adding coagulant, ozone and their combination. The
 285 results showed that feeding the Class A water directly to the ceramic membrane led to rapid
 286 fouling as observed from the rapid rise in TMP to 1.4 bar within 10 h of filtration time for
 287 130 L/(m².h) flux operation. The fouling rate for direct Class A water increased from 0.64 to
 288 1.6 bar/h at the first (1st) and last (17th) filtration cycle respectively.

289



290

291 **Figure 1:** TMP rises as a function of time for direct Class A feed, coagulant feed, ozone feed
 292 and ozone-coagulant feed (a) and UVH-10 min, UVH-30 min and UVH-10 min-coagulant
 293 feed (b). All fluxes were fixed at 130 L/(m².h).

294

295

296 Under the same operating conditions, when 3 mg (as Al³⁺)/L of polyaluminium chloride
297 (PACl) coagulant was dosed prior to the membrane, TMP rise was reduced. Compared to
298 direct Class A feed, TMP rose more slowly and approached 0.68 bar for the same volume of
299 water filtered. The reduction was mostly associated with reduced rises between backwashes.
300 When ozone only was added to the feed water, the TMP showed a reduced rise between
301 backwashes initially. Using either coagulant or ozone, the gradual build-up of TMP over the
302 course of the run appeared similar to direct Class A water feed. In the case of ozone, it has
303 been recently reported that reduced TMP rise between backwashes could be due to the
304 reduced flow resistance in the oxidised organic matter accumulated on the membrane surface
305 [9]. However, when ozone and coagulation are combined, both overall and between backwash
306 TMP rises were greatly reduced. The finding is supported in pilot trials of CMF on recycled
307 wastewater where ozone was observed to reduce the TMP rise during filtration while
308 coagulation reduced TMP rise after each backwash [1, 2]. Using the data in Figure 1 and
309 Equation 1, change in fouling rate can be calculated to compare performance. The fouling
310 rate increases by up to 150% during the 10 h filtration period for the direct Class A water. In
311 the case of ozone, this reduced to 112%, indicating for the chosen flux of 130 L/(m².h) fouling
312 was increasing. When coagulant was instead applied, the change in fouling rate was similar.
313 However the change in fouling rate reduced significantly to 27% with the combined ozone-
314 coagulant feed to the ceramic membrane. Coagulant and ozone thus inhibit the need for
315 chemically enhanced backwashes which remove irreversible foulants that cause accelerated
316 fouling rates [3]. The result here confirms the well-known effect of greatly enhanced
317 sustainable fluxes following coagulation and ozonation and the filtrate is suitable for
318 downstream RO processing.

319 Figure 1b demonstrates the TMP profile of each process operated at 130 L/(m².h) flux for direct
320 Class A feed and feed pre-treated with UVH and combined UVH and coagulation process.
321 Longer UV treatment time from 10 minutes to 30 minutes greatly reduced TMP rise between
322 backwashes, which could be due to similar reasons of reduced filter cake resistance as observed
323 for ozone [9]. Spikes in TMP were observed for some filtration cycles from the 10 minute UVH
324 (UVH-10 min, Fig. 1b), exceeding the TMP of direct Class A feed between 3 and 7 hours. This
325 however was considered to be due to experimental issues, for example air accumulation in the
326 membrane tube which was removed during backwash. Importantly however, TMP rise rate
327 between backwashes was consistently lower than direct Class A highlighting the reduced filter
328 cake resistance. Coagulation was only added to the 10 minute UVH case as it showed a near
329 complete removal of TMP build-up in the 10 hour test period. The effect appears similar to that
330 for ozonation – coagulation treatment. The change in fouling rate was approximately 20%,
331 which is similar to the ozone-coagulant treated water.

332 The HIFIs shown in Table 2 show the normalised quantitative differences between the CMF
333 filtration scenarios, where any oxidation process leads to significantly reduced fouling when
334 used in conjunction with coagulation. Although either may be suitable, previous studies
335 directed to RO membrane fouling benefits found UVH more expensive than ozone [15]
336 suggesting the importance in considering cost in deciding to use either ozone or UVH.

337

338

339

340 **Table 2.** HIFI on CMF for each pre-treated water

Pre-treatment	CMF HIFI (m²/L)
Direct Class A	2.75
Coagulation	2.08
Ozone + Coagulation	1.25
UVH-10min + Coagulation	0.37

341

342 *Ceramic membrane treatment performance*

343 The measured quality indicators of the untreated Class A water feed and the various pre-
 344 treatments options are shown in Table 3. Originally, the feed water showed relatively high
 345 DOC and low UV₂₅₄ absorbance. DOC removal was <10% for coagulation, ozone or UVH, but
 346 when coagulation was combined with oxidation, DOC removal increased to 10% for
 347 UVH+coagulation, and 18% for ozone+coagulation possibly by ozone enhanced coagulation
 348 effects [42]. Coagulation reduced UV₂₅₄ absorbance by only 13%, but any combination with
 349 oxidation led to significant reductions between 44% and 63%, where the highest was measured
 350 in the ozone cases.

351

352 **Table 3.** Measured water quality indicators after various pre-treatment options prior to CMF

Pre-treatment	UV₂₅₄ (1/m)	pH	DOC (mg/L)	SUVA (L/(mg·m))
None (direct Class A)	16	7.43	9.1±0.4	1.74
Coagulation	14	7.53	8.3±0.3	1.70
Ozone	7	7.44	8.4±0.6	0.88
Ozone+coagulation	6	7.39	7.5±0.1	0.78
UVH	9	7.51	8.6±0.2	1.02
UVH+coagulation	8	7.57	8.2±0.4	1.02

353

354 Organic fractions within the various pre-treatment options stages were analysed more closely
 355 by LC-OCD and the results are shown in Figure 2. The LC-OCD analysis enables the
 356 quantification of organic matter fractions including biopolymers (MW>>>20,000 g/mol), humic
 357 substances (MW~1000 g/mol), building blocks (MW 300-500 g/mol), low molecular weight
 358 (LMW) substances (MW <350 g/mol) which are the sum of low molecular weight neutrals and
 359 low molecular weight acids. The results show that feed water dissolved organic material
 360 consisted of 47% humic-like substances, 17% LMW substances, 14% building blocks, 12%
 361 biopolymers and 10% hydrophobic organics. Membrane filtration (Figure 2a) removed mostly

362 the biopolymer proportion (60% removal) due to their high molecular weight and their sticky
363 properties. Humic substances were almost similar in concentration in the membrane permeate
364 and the feed. They can readily pass through the membrane pores of 0.1 μm in size. A small
365 fraction of large humic substances might be retained due to tortuosity effects. For the smaller
366 components (building blocks and LMW organics) slight increases were observed, which cannot
367 be explained and may be due to sample handling.

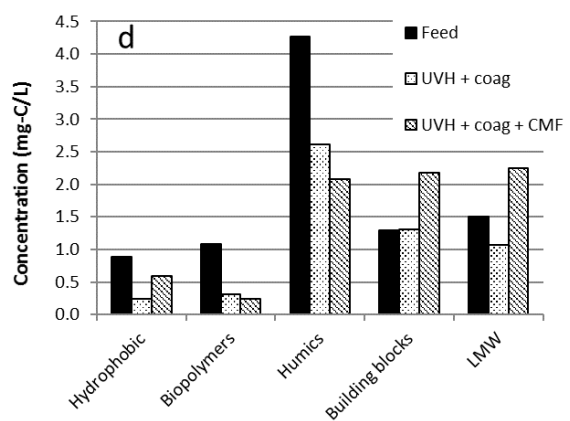
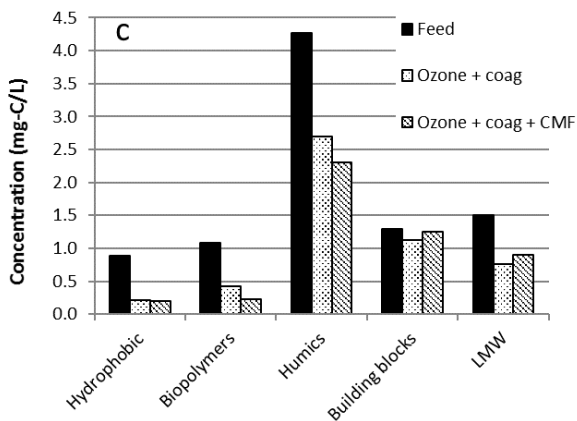
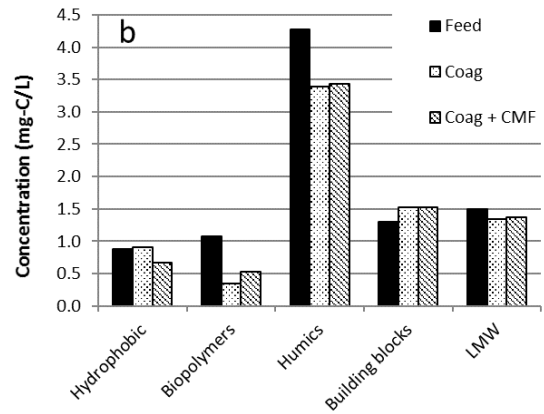
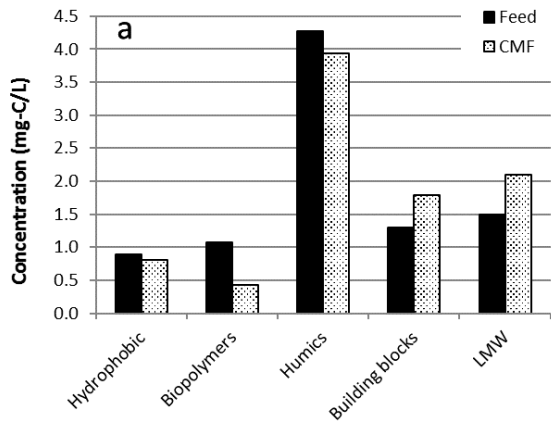
368 Considering the results with the pre-treatment options prior to CMF biopolymer removals of
369 68%, 60% and 71% for coagulation, ozone+coagulation and UVH+coagulation treatments
370 were observed respectively. Biopolymers are readily removed by coagulation [6] whereas
371 oxidation processes result in a breakdown of the large molecules and production of smaller
372 molecules which are harder to be removed by coagulation observed only in the case of ozone.
373 At the first glance it seems that ozonation was more effective in breaking down the
374 biopolymers. However, due to the single sample analysis, it is questionable whether that effect
375 is significant. Application of CMF to complete these pre-treatment options did not contribute
376 to large additional differences in the biopolymer concentrations.

377 Removal of humic substances prior to CMF also occurred in all cases, but was highest in both
378 oxidation cases (Figures 2c and d) at about 40% as opposed to 21% for just coagulation.
379 Application of CMF did not appear to offer humic substances removal applied directly to the
380 feed or after coagulation, but some additional removal occurred after oxidation, leading to a
381 total humic substances removal of about 50% for both ozone and UVH cases. In the case of
382 building blocks, no noticeable concentration changes due to the pre-treatment prior to CMF
383 were observed. However, unexpectedly concentrations of the LMW fractions were lower for
384 ozone and UVH than coagulation alone. Previous studies on ozone and UVH reaction with
385 wastewater organics coming from the conventional activated sludge process had shown
386 increases in the proportion of LMW acids [8]. The LMW acids make up the LMW fractions
387 presented in Figure 2, and no increase was observed in our case potentially due to the lower
388 relative doses of ozone and UVH where LMW acid formation is lower. Also, while the
389 concentration of humic substances was similar in their work, our water contained less of the
390 other organic fractions and therefore had a different initial organic profile highlighting the
391 differences between various wastewater sources.

392

393

394



395

396

397 **Figure 2:** DOC fractionation after various stages within the pre-treatment options of CMF only
 398 (a), coagulation+ CMF (b), ozone+ coagulation + CMF (c) and UVH+ coagulation + CMF (d).

399

400 When pre-treatments were used with CMF the membrane generally showed little change to the
 401 relative profile of organics. This is expected due to the relatively large pore size (0.1 μm), but
 402 in the case of CMF on its own (Figure 2a), the larger biopolymer molecules were rejected by
 403 the membrane. As mentioned earlier, oxidation assisted the CMF to remove additional humic
 404 substances. The only other exception was in the case of UVH, which showed unusually high
 405 levels of building blocks and LMW organics in the permeate compared to the CMF feed. The
 406 reason for this is unknown since the membrane is not expected to increase any organic fraction
 407 unless it could come from particle organic matter as a result of advanced oxidation UVH.
 408 However this would be the case if also seen in the UVH+coagulation sample. Contributions to
 409 LMW fraction by oxidation of other dissolved organic fractions is also known [8], but is not
 410 expected to have occurred in just this test with CMF, particularly since this effect occurs only
 411 in very high UVH doses as compared to here. The potential for adsorbed organics to be released
 412 from the membrane due to oxidation is also ruled out because the samples were taken in batch
 413 from the oxidation process to the CMF test unit (enough time for residual oxidants to be
 414 consumed prior to contacting membrane). This increase is therefore unexpected and because
 415 only one sample was analysed, it may relate just to the experimental or preparation of this
 416 sample.

417

418 Considering differences between ozone and UVH, González et al [8] reported ozone and UVH
419 techniques lead to different impacts on the organic fractions as also assessed by LC-OCD. In
420 the case of ozone in Figure 2c, the effect in addition to coagulation (Figure 2b) showed its
421 selective nature participating in removal of humic substances and LMW organics. Low
422 biopolymers in CMF and coagulation+CMF cases were consistently lower in oxidised samples
423 hence the oxidation process (including peptide bond cleavage and depolymerisation of
424 polysaccharides) did not lead to any observed breakthrough of biopolymer substances (proteins
425 and polysaccharides) to the CMF permeate. Ozone is also known to react preferably with the
426 highly aromatic humic substances, and the slightly aromatic and hydrophobic LMW neutrals
427 [43]. As shown in Figures 2c and d, the oxidation processes can also be seen to increase the
428 hydrophilicity of the DOC, where no large removal of the hydrophobic organic fraction was
429 observed in CMF and coagulation+CMF cases, while oxidation led to 34% to 77% removal
430 across all the pre-treatment steps. In terms of aromaticity, oxidation led to a large reduction as
431 indicated by the SUVA results shown in Table 3. Although the humic substances were the
432 mostly dominant organic fraction after pre-treatment, the oxidation processes are expected to
433 deplete the aromaticity of these organics by attack of double bonds and aromatic rings but not
434 to cleave them leading to structure loss, unless high oxidation doses are used where LMW
435 fractions are observed to increase [8]. The resistance of humic substances to oxidation has been
436 proposed to be associated with steric obstruction preventing cleavage of the core molecular
437 bonds of humic structures [44]. These changes in chemical composition, together with their
438 lower overall relative abundance, could lead to the reduced fouling of RO membranes observed
439 previously [15, 16] and is expected to greatly alter the biofouling propensity. Both will be
440 explored later in this paper.

441

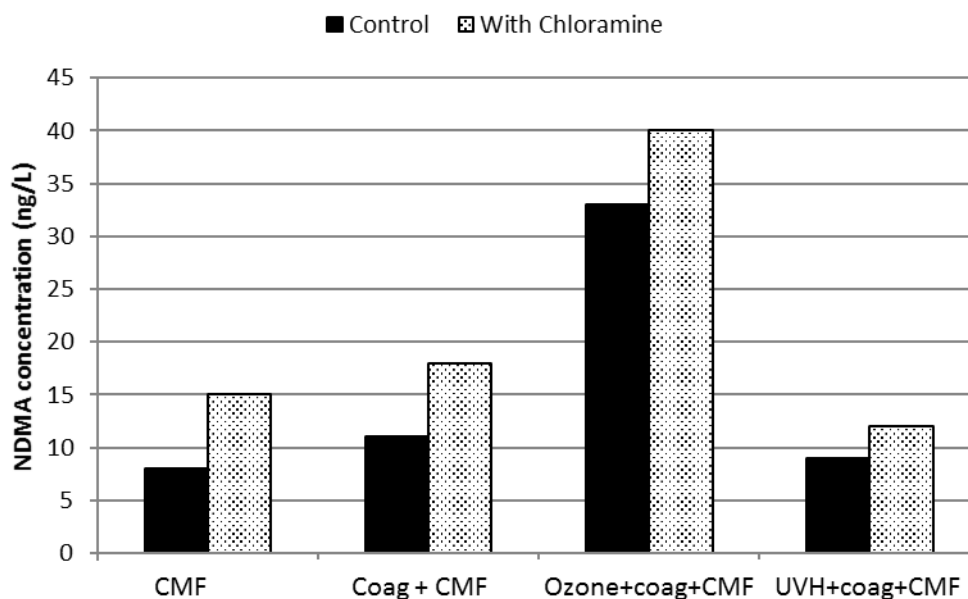
442 *N-nitrosamines analysis of ceramic membrane permeate*

443 Figure 3 shows NDMA concentrations observed after the various ceramic membrane pre-
444 treatment processes. NDMA was detected in the CMF only treated water at 8 ng/L.
445 Coagulation+CMF showed a slightly higher NDMA concentration at 11 ng/L, while
446 ozone+coagulation+CMF caused a large increase to 33 ng/L. UVH+coagulation+CMF on the
447 other hand showed a concentration of 9 ng/L, being similar to the CMF or coagulation+CMF
448 treated waters. Chloramine dosing tended to increase NDMA concentrations in any sample
449 by 7 ng/L, except for UVH which increased only by 3 ng/L. Ozone is important to achieving
450 the desirable high CMF fluxes, but clearly its impact to form NDMA is more critical than
451 chloramine which may be used to control RO membrane biofouling. Oxidation is known to
452 greatly reduce the potential for NDMA formation in drinking water application [45] however
453 ozone also induces NDMA formation when applied to wastewater. 7 out of 8 wastewater
454 treatment plants surveyed for DBP formation associated an increase in NDMA as a result of
455 the ozonation stage [46]. Biological filtration following ozone assisted in removing formed
456 NDMA. In the same work, the O₃/DOC mass ratio was analysed, where plants showed ratios
457 ranging from 0.2 to 1.5 w/w. In our case, the ratio was 1.4 w/w as ozone dose was 13 mg-

458 O₃/L and DOC was 9.0 mg-C/L, which is at the higher end of their reported range. While this
 459 higher DOC supports the ability for ozone to form NDMA, their survey of various plants
 460 found no conclusive link to O₃/DOC mass ratio, where instead NDMA formation is more
 461 likely dependant on the presence of precursors in the wastewater and the extent of treatment
 462 by the upstream treatment plant. Krasner et al. [47] reported that NDMA can form during
 463 ozonation of a limited group of tertiary amine precursors present in drinking water (including
 464 wastewater impacted source waters), although the association between ozonation and NDMA
 465 formation has not yet been found.

466 The issue of increased NDMA formation from application of ozone upstream of RO has been
 467 considered previously [15], where the reduced NDMA formation potential by ozone was not
 468 offset by its role in producing NDMA. It was concluded that this will be important in
 469 applications where NDMA concentration is monitored, for example potable reuse. Use of
 470 UVH to avoid NDMA in such applications may offset the potentially higher costs mentioned
 471 earlier. Optimisation of the UV and H₂O₂ dose may find a means to achieve the desired
 472 oxidation with lower energy [34]. The result in Figure 3 suggests that for consideration of the
 473 use of the recycled water, the choice of oxidation to achieve high CMF fluxes will have a
 474 strong impact on NDMA formation while chloramine dosing will have less of an effect.

475



476

477 **Figure 3:** NDMA concentration measured for both control and chloraminated samples of
 478 feed waters (dosed with 4 mg/L pre-formed chloramine) pre-treated with CMF,
 479 coagulant+CMF, ozone+coagulant+CMF and UVH+coagulant+ CMF. Chloraminated waters
 480 used as RO feeds.

481

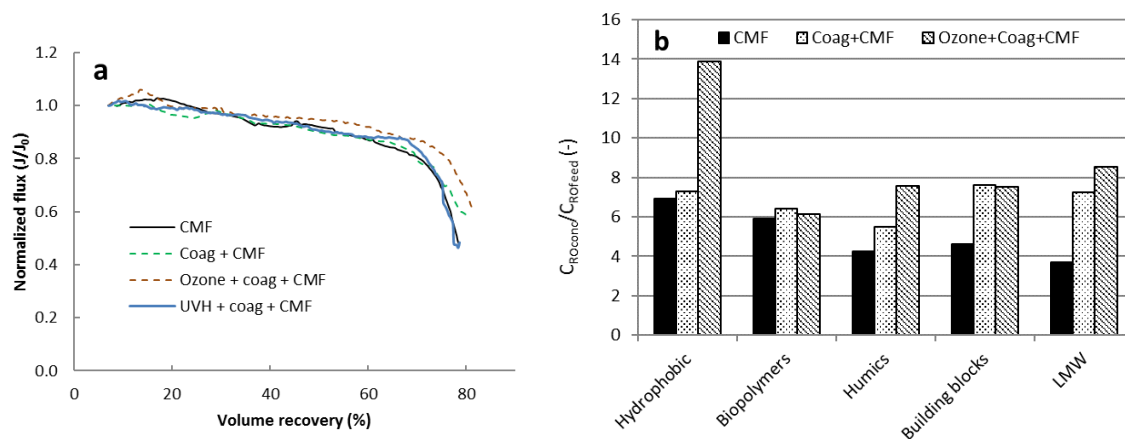
482

483 *Impact of CMF pre-treatments on downstream RO*

484 RO performance during fouling loading

485 The effect of fouling of the RO membranes pre-treated by CMF, coagulation+CMF,
 486 ozone+coagulation+CMF and UVH+coagulation+CMF was compared and the data is shown
 487 in Figure 4. In these cross-flow batch concentration runs, similar flux decline results were
 488 observed for all pre-treatment modes indicating the accumulated fouling under any water feed
 489 did not show differences in resistance of water flux through the membrane. The decline
 490 experienced by all samples is likely due to the increasing salinity and in turn osmotic pressure
 491 which reduces the flux. A slight benefit to performance, however, was observed for the
 492 ozone+coagulation+CMF pre-treated water where the drop off in flux occurred at a slightly
 493 higher recovery than the other samples. Previous research showed strong benefits of ozone or
 494 UVH to prevent increasing flux resistance through the RO membrane between 70 and 120
 495 hours of testing [34]. A key difference in our study was application of oxidation prior to
 496 membrane filtration, where the CMF must follow from oxidation in order to achieve the high
 497 flux effect. Oxidation in our case can therefore react with additional organics (i.e. biopolymers)
 498 that are removed by membrane filtration (Figure 2), and may have minimised the differences
 499 to RO fouling resistance. However, unlike the previously reported benefits of oxidation and
 500 the slight benefit from our testing with ozone, we did not see any benefit to RO membrane flux
 501 as a result of UVH. Therefore based on our short term test result, applying oxidation prior to
 502 CMF shows no significant advantage to RO membrane flux as a result of altered
 503 organic/inorganic fouling properties. .

504



505

506 **Figure 4:** Normalized flux decline versus permeate recovery (%) for various feeds (a) and
 507 ratio of concentrations of the various organic groups between RO concentrate and RO feed,
 508 C_{ROcond}/C_{ROfeed} , with various pre-treatments determined by LC-OCD (b).
 509

510 The RO test aimed to simulate a RO plant where in a single housing, a series of elements (e.g.,
 511 7 elements) operating at effectively the same pressure at a given moment in time within the
 512 vessel have decreasing fluxes along the length of the vessel as a function of the concentration
 513 (water recovery). Lead elements have higher flux than tail elements. However, the fouling on
 514 the membranes in the bench setup differs from the real plant in that it is the same membrane

515 tested from the initial water rejected (lead element) to the final rejection (tail element). Fouling,
 516 (including biofouling) on lead and tail elements has been investigated in pilot sea water and
 517 wastewater RO plants showing very different behaviour unique to the fluxes and brine
 518 concentrations that differ greatly along the membrane pressure vessel [48]. Respecting these
 519 differences that are more difficult to replicate at bench scale, the test conducted here
 520 conveniently and quickly shows the average fouling across all elements. Tail elements with
 521 higher brine concentrations (70% recovery) were shown to have higher degree of mineral
 522 scaling over biofouling [48]. Therefore, the foulant here represents accumulated organic and
 523 inorganic substances across the entire rejection range.

524 EC for both RO concentrate and permeate at 80% volume recovery are summarised for each
 525 pre-treated water type (with CMF) in Table 4. Prior to testing with samples, benchmark
 526 rejection of 99.5% was confirmed using 2000 ppm NaCl at 15.5 bar for 15% recovery. Looking
 527 at the permeates from sample testing, higher EC from oxidised samples was observed which
 528 was related to the higher concentrations of the feeds used and not due to changes as a result of
 529 ozone. This finding is supported by previous pilot trials which found no change in salt transport
 530 through the membrane due to altered chemical properties as a result of upstream ozone
 531 treatment [15]. They also concluded that the ozone did not deteriorate the RO membrane as a
 532 result of this observation after 3000 hours of pilot testing due to rapid quenching of ozone by
 533 the organic and mineral components of the wastewater such that no harmful residual entered
 534 the RO membrane unit.

535
 536 **Table 4:** EC for RO feeds from various pre-treatments, as well as the concentrate and
 537 permeate collected at the end of the runs

Pre-treatment	RO feed ($\mu\text{S/cm}$)	RO concentrate ($\mu\text{S/cm}$)	RO permeate ($\mu\text{S/cm}$)
CMF	1298	5470	82
Coagulation+CMF	1298	6660	76
Ozone+coagulation+CMF	1326	6130	158
UVH+coagulation+CMF	1348	5560	102

538
 539 An increase in permeate conductivity due to charged organics from oxidation diffusing through
 540 the membrane was also not likely, where previous testing on two wastewater sources found
 541 similar or slightly lower DOC concentrations in RO permeates for ozone+CMF treated
 542 wastewaters compared to untreated wastewater feeds [17]. Due to the focus in this work on the
 543 process train performance and membrane fouling, further analysis of the RO permeate was not
 544 conducted but would be an interesting suitable topic for future work to compare the differences
 545 between the processes.

546 Potential depositions on the RO membrane could be explored by observing the organic
 547 fractions concentration factors presented in Figure 4b (concentration ratio in the RO

548 concentrate, C_{ROconc} , to the feed, C_{ROfeed}). Factors of 5 would be expected for volume recovery
549 of 80% if little permeated the membrane, or came out of solution (either by precipitation in the
550 system or deposition on the membrane). However, the ratios were instead mostly around 7 and
551 lower, suggesting that the recovery based on the concentration ratio was closer to 85%. The
552 exception to this was the very large ratio (13.9) for the hydrophobic organics in
553 ozone+coagulation+CMF pre-treated water which will be discussed later.

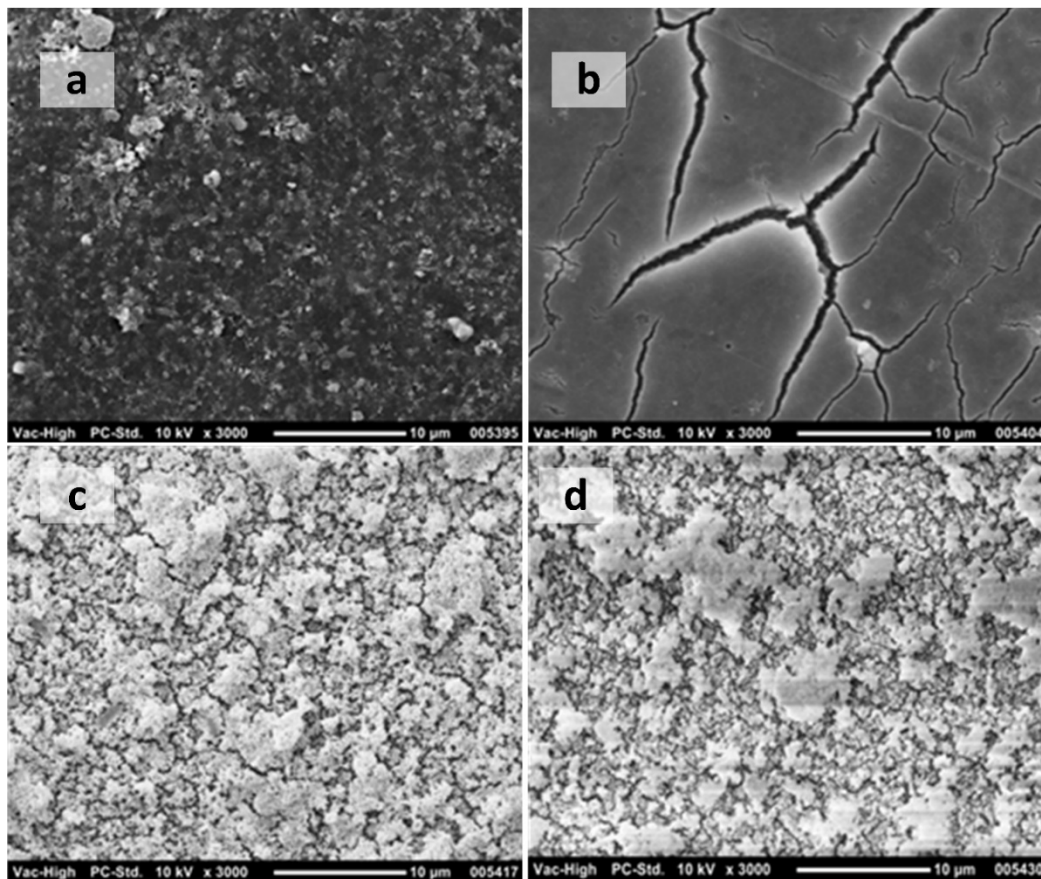
554 The hydrophobic fraction ratios was similar for CMF only (6.9) to coagulant + CMF (7.3), and
555 close to the concentration ratio around 7 indicating little permeation or deposition of these
556 fractions. Ozone+coagulation+CMF showed a very high ratio (13.9) where C_{ROfeed} was low due
557 to oxidation, but increased more than the RO concentration factor. It cannot be concluded from
558 the present data if this was due to an effect to increase hydrophobic property of organics due
559 to concentrating, or sensitivity of the ratio to low feed concentration of hydrophobic organics
560 (0.2 mg-C/L). Looking at biopolymers, all ratios were much closer between 5.9 and 6.4, and
561 lower than the concentration ratio of ~ 7 . Due to their high molecular weight, biopolymers are
562 not expected to permeate the membrane and therefore it is suggested they are deposited within
563 the concentrate cycle including depositing on the membrane. In all pre-treatment cases, it is
564 possible that biopolymers contributed to membrane organic fouling. Humic substance
565 concentration ratios on the other hand were different in all RO pre-treatment cases. For CMF
566 only, a lower ratio of 4.3 for humics can be seen suggesting their limited ability to concentrate
567 and potential to deposit on, or diffuse through, the membrane. With coagulation+CMF, then
568 ozone+coagulation+CMF, progressively higher increases in humic substance proportions
569 reaching the concentration expected for reduced deposition, or complete rejection, by the
570 membrane. This is especially the case when they were reacted by ozone where it approached
571 the system concentration ratio of ~ 7 . Building blocks and LMW organics, which showed higher
572 deposition on, or passage through, the RO membrane with just CMF and in turn lower increase
573 in the RO concentrate, suddenly reached the full concentration factor apparently due just to
574 coagulation. Their association with coagulant appears to have inhibited their ability to attach
575 to or transport through the membrane, and they instead concentrate in the RO brine.

576

577 SEM images of the membrane surface taken at the end of the RO treatment process are shown
578 in Figure 5. An SEM image of the original RO membrane is presented in the Supplementary
579 Material Figure S3 for reference. The images of the fouled RO membranes show that each
580 treatment type used in conjunction with the ceramic membrane led to very different structural
581 features of the fouling layer deposited on the RO membranes. CMF pre-treated water led to a
582 uniformly grainy textured material, with particles around 0.55 μm and less in diameter
583 appearing embedded within a smooth polymeric-like material. The particles may have
584 originally been small enough to permeate the 0.1 μm CMF membrane, and agglomerate on the
585 RO membrane surface. When coagulation+CMF pre-treated water was used, a very smooth
586 texture appeared with no visible particles. It appears the application of coagulant facilitated
587 removal of the particulate matter by the ceramic membrane. The fouling layers of the
588 ozone+coagulation+CMF and UVH+coagulation+CMF pre-treated water were similar to each
589 other and very different to CMF or coagulation only pre-treatments. They uniquely showed a

590 grainy texture of highly variable agglomerates of $<1\ \mu\text{m}$ to several μm in size. It appears that
591 the material that permeated through the CMF after oxidation by ozone or UVH formed
592 aggregated structures rather than a smooth, continuous gel layer as observed for coagulation or
593 direct filtration of the wastewater. A different result was observed on bench and pilot tests
594 where RO membranes were fouled with ozonated MBR filtrate. While dense fouling layers
595 were also observed with original (not oxidised) wastewaters, the fouling layer from the
596 ozonated wastewater was also more open [16], but did not show a grainy texture as observed
597 here. This may relate to differences in the wastewater, ozone dose approach, and final water
598 recoveries. Aggregation of biopolymers following ozonation has been observed by Yu et al for
599 synthetic water systems [9]. The aggregates were used to explain mechanisms of reduced or
600 increased fouling of a 10 to 20 nm UF membrane as a result of increasing sizes of alginate and
601 model protein BSA, respectively. While the focus of their work was the fouling of the UF
602 membrane, their results showed the aggregation mechanisms which could relate to organics in
603 the CMF permeate which will be fed to RO.

604



606 **Figure 5:** SEM images of fouled RO membranes, including membrane fouled with CMF only
607 treated water (a), with coagulation + CMF (b), ozone + coagulant + CMF and (c) UVH +
608 coagulation + CMF (d). Original membrane without fouling shown in Supplementary Material
609 Figure S3.

610

611 At the end of the RO experiments (i.e., after 80% volume recovery), the membranes were rinsed
612 with clean water and clean water flux was measured. When rinsing with clean water the loosely
613 attached foulants could be expected to detach during hydraulic cleaning, and reversible fouling
614 is a measure of flux that could be restored after hydraulic cleaning. Clean water fluxes of 8.6,
615 20, 16 and 13 L/(m².h) were measured for membrane previously exposed to CMF,
616 coagulation+CMF, ozone+coagulation+CMF and UVH+coagulation+CMF pre-treated feeds,
617 respectively. The higher clean water flux represents higher fouling reversibility, comparing to
618 the new membrane clean water flux of 22 L/(m².h) as shown in Figure S4 in the Supplementary
619 Material. Therefore, the action of coagulation (together with ozonation and UVH treatment),
620 on the organics leads to greater fouling reversibility on the RO membranes. Coagulation on its
621 own was most superior in reversing fouling, while either oxidation in addition to coagulation
622 showed less reversibility. This may be due to texture differences of the oxidised foulants as
623 shown in Figure 5, or potentially their chemical differences, where less fouling material was
624 removed due to simple water rinsing. The ability of clean water to more easily remove fouling
625 matter after ozone application (without coagulant) was also found by Zhang et al. [17]. In
626 practice, a treatment process that leads to high membrane fouling reversibility suggests that
627 less intensive chemical cleaning will be required for the downstream RO membranes.

628

629 Biofouling potential tests

630 Table 5 shows the BDOC test results specifically for waters pre-treated to be fed to RO. No
631 significant change in BDOC was observed between CMF or coagulation+CMF pre-treatment.
632 BDOC however increased after ozone, ozone+coagulation, UVH and UVH+coagulation prior
633 to CMF pre-treatments. This indicates that the oxidation processes used to increase CMF flux
634 lead to increased biodegradability, and in turn increases the potential for biofouling if fed
635 directly to RO as proposed in our work. It is more common in practice for biological filtration
636 to follow oxidation especially to avoid the biofouling risk [49]. For example a biologically
637 activated carbon (BAC) filter was installed between the ozone-ceramic membrane and RO
638 processes, and found to remove 30% to 50% of the DOC [19] and no biofouling issues were
639 identified over 9 months of operation [18]. However, the focus of this work was to assess the
640 potential for biofouling where BAC pre-treatment before RO may not be required, and
641 increased ability to assimilate organics may not directly correlate to the ability for a biofilm to
642 form on the RO membrane.

643

644

645

646

647

648 **Table 5.** Biodegradability of water samples after various pre-treatments, including those used
 649 as feed to RO

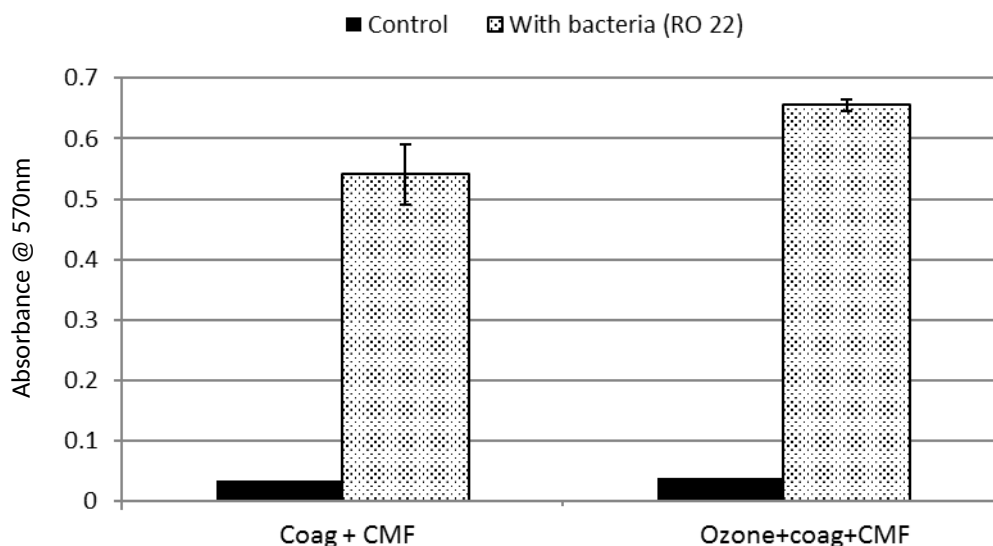
Pre-treatment	BDOC mg/L	RDOC* mg/L	DOC mg/L	BDOC % of DOC
CMF	0.50	7.83	8.33	6.0
Coagulation+CMF	0.49	7.87	8.36	5.9
Ozone +CMF	1.34	6.46	7.80	17.2
Ozone+ coagulation +CMF	1.17	6.11	7.28	16.1
UVH+CMF	1.11	6.82	7.93	14.0
UVH+coagulation+CMF	1.08	6.75	7.83	13.8

650 *RDOC = Refractory dissolved organic carbon = Total DOC – BDOC

651

652 Bioassay results

653 The bioassay analysis showed that the concentration of bacterial cells in the
 654 ozone+coagulation+CMF treated water was ~ 20% higher than coagulation+CMF treated
 655 water (Figure 6). The results also suggest that bacteria can grow in a liquid medium of
 656 ozone+coagulation+CMF treated water, which could be rich in assimilable carbon (and
 657 potentially nutrients) compared to coagulation+CMF treated water since more biodegradable
 658 organic carbon is present. This confirms the BDOC finding, where more DOC was removed
 659 by biological activity. However, improved assimilability of organics does not directly indicate
 660 RO biofouling as attachment of cells to the membrane surface and formation of a biofilm,
 661 rather than BDOC only, decides whether the water has more or less ability to facilitate
 662 biofouling.



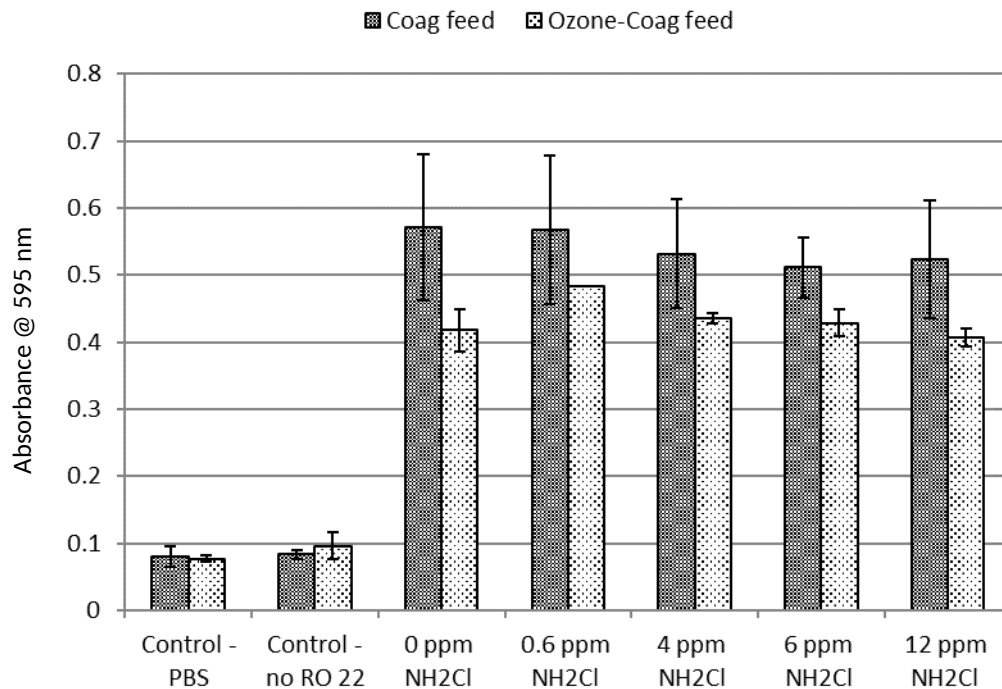
663

664 **Figure 6:** Absorbance measurement at 570 nm of RO 22 bacteria suspension of each water.
 665 Error bars show standard error calculated form the standard deviation.

666

667 Figure 7 shows the absorbance of biofilm after removing the bacterial suspension for control,
668 coagulant and ozone-coagulant feeds after 48 h. The preformed chloramine (NH_2Cl) was
669 dosed at different concentrations to the feed samples with bacteria (RO 22) to observe its
670 effect on inhibiting growth of the biofilm. It was observed that the presence of biofilm growth
671 was slightly less for ozone-coagulation treated water compared to coagulation alone treated
672 water as indicated by lower light absorbances. Interestingly, the biofilm assay showed
673 chloramine had no measurable impact on the biofilm growth control or its removal. However,
674 its known application to control biofouling in RO membranes may work differently to
675 inhibiting biofilm growth which are discussed later during the accelerated RO biofouling
676 tests.

677 Another interesting feature of the crystal violet assay was the consistently lower biofilm
678 formation when ozone was used. While it was observed that cell growth is enhanced in the
679 presence of water that was treated by ozone (Table 5 and Figure 6), the formation of an actual
680 biofilm which is responsible for biofouling of RO membranes appears suppressed. Biofouling
681 is a complex phenomenon, and recent research has shown that MF pre-treatment of
682 wastewater leads to enhanced biofilm formation [23]. This was found to be due to the removal
683 of ‘antibiofilm’ substances that inhibited growth of the model bacterium *Pseudomonas*
684 *aeruginosa PAO1*. The MF membrane allowed the passage of lectin-like humics which were
685 able to attach to the RO membrane to form a conditioning layer which in turn facilitated
686 bioadhesion. In our case, it is possible that the lectin-like humic substances were significantly
687 altered by ozone action which reduced their ability to form the essential conditioning layer
688 needed for biofilm establishment. Indeed as shown earlier, ozone action on organics reduced
689 the proportion of humic and hydrophobic substances (Figure 2c) and reduced aromaticity
690 (Table 3). Also, it was noted during analysis of the RO concentrate (Figure 4b), that humic
691 substances can deposit on, or permeate into, the RO membrane which implies they can attach
692 to the polyamide membrane material and further facilitate bioadhesion. The action of ozone
693 to alter their properties limited their ability to be transported through the CMF membrane
694 (Figure 2c), but also apparently improved their ability to be rejected by the RO membrane
695 (Figure 4b).



696

697 **Figure 7:** Crystal violet assay measurement at 595 nm for cell density and biofilm
 698 production by each water. Error bars show standard error calculated from the standard
 699 deviation.

700

701 *Accelerated RO biofouling test*

702 RO membranes were tested for accelerated biofouling in a cross flow system of two selected
 703 water solutions spiked with RO22 bacteria: coagulation+CMF with chloramine (dosed 2
 704 hours prior to finishing the RO test) and ozone+coagulation+CMF without chloramine
 705 dosing. A control with chloramine dosing but no RO22 bacteria was also run. The results of
 706 the tests showing the thickness of the fouling layers formed measured by confocal microscopy
 707 are presented in Table 6. The addition of RO22 led to additional fouling from biofilm growth
 708 on the RO membranes, despite the addition of chloramine. This further supports the crystal
 709 violet assay result in Figure 7 where no change in biofilm formation was observed as a result
 710 of chloramine dosing. The solution treated with ozone showed slightly thicker fouling layer
 711 thickness compared to coagulant only. The thickness of the fouling layer in Table 6 was
 712 greater than without ozone, which is the opposite trend to that in Figure 7 which may be due
 713 to differences between composite fouling layers and biofilms, as well as effects of permeation
 714 and cross flow that occur in the case of RO operation. The differences in the results of the RO
 715 biofilm for the crystal violet assay will be now looked at more closely using confocal
 716 microscopy to observe the abundance of bacterial cells within the biofilm.

717

718 The confocal images presented in Figure 8 show the presence of live (green) and dead (red)
 719 cells. In the Figure, x represents the distance from the RO membrane surface, and l represents
 720 the estimated total fouling layer thickness from Table 6. The ratio x/l is therefore the relative
 721 distance from the RO membrane surface to the fouling layer surface facing the flowing
 722 solution. A few live (green) cells appeared on the control membrane without the addition of
 723 RO 22, reflecting the presence of low levels of bacteria in the system. In experiments with
 724 spiked RO22, many more cells were observed on the membranes. Looking more closely we
 725 can see varying quantities and proportions of live and dead cells as a function distance from
 726 the membrane surface. For the membrane with coagulant only and chloramine added 2 hours
 727 prior to finishing the RO run, live and dead cells were seen near the top of the fouling layer
 728 facing the flowing solution at $x/l = 0.93$ (Supplementary Material Figure S6). Readily
 729 available chloramine in the solution was potentially responsible for killing these sessile
 730 bacteria. Going deeper to near half the fouling layer thickness ($x/l = 0.47$) in Figure 8 we again
 731 see a proportion of both dead (red) and live (green) cells. Closer to the membrane surface (x/l
 732 $= 0.20$ in Figure 8), there were predominantly green (live) cells suggesting that chloramine
 733 was not effective for killing these cells, possibly because they were sheltered by the fouling
 734 layer above. From the thickness of 4 μm to the membrane surface, cells were predominantly
 735 dead (red) (observed at $x/l = 0.07$ in Figure 8), indicating that the cells that first attached to
 736 the membrane surface did not survive during the run, potentially as a result of depletion of
 737 nutrients required for cell growth as the water diffuses through the fouling layer. Right at the
 738 membrane surface ($x/l = 0$) no cells were found. This could potentially be the conditioning
 739 layer, having a thickness of around 2 μm .


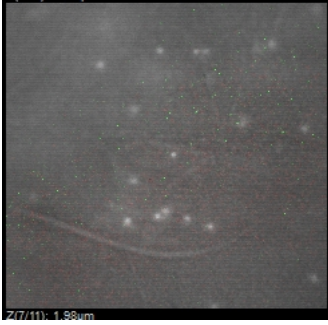

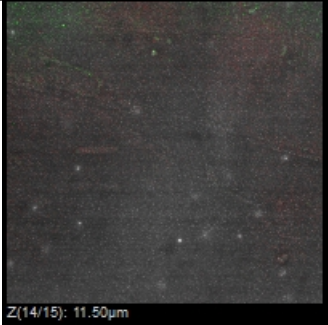
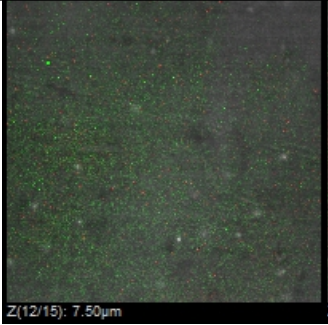
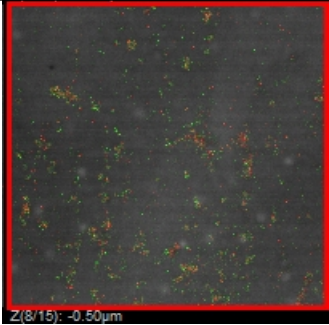
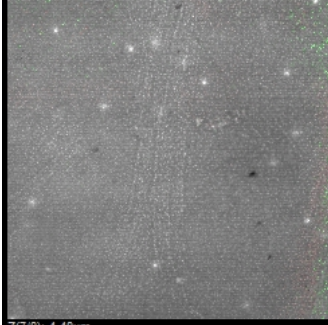
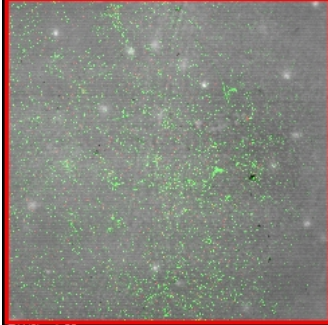
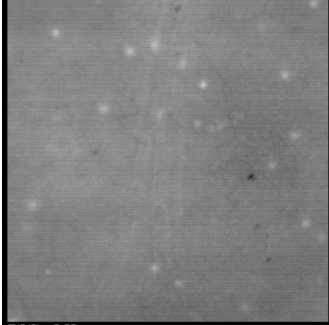
740 In the case of ozone treated water (without chloramine) no cells were seen from the top of the
 741 fouling layer facing the flowing solution down to $x/l = 0.33$ as shown in Figure 8. However
 742 reaching $x/l = 0.27$ saw abundant numbers of predominantly live (green) cells. Like the
 743 coagulation pre-treated RO feed, few cells were seen 2 μm from the RO membrane surface
 744 ($x/l = 0.06$), but some dead cells appeared at 4.0 μm (Supplementary Material Figure S7). So
 745 despite the thicker fouling layer in the presence of ozone treated water as measured by
 746 confocal microscopy, it appears the microbial population was much more limited in its
 747 thickness compared to the coagulant+CMF pre-treated water case.

748

749 **Table 6:** Fouling layer thickness measured after 22 h cross flow RO run with different water
 750 samples spiked with RO22 bacteria. Chloramine added 2 hours prior to completion of the RO
 751 test (except for ozone-coagulant where no chloramine was dosed).

Water sample	Biofilm thickness, l (μm)
Coagulant only (control with no RO22 and with 4 mg/L chloramine)	18
Coagulant only (RO22 with 4 mg/L chloramine)	30
Ozone-coagulant (RO22 no chloramine)	36

752

	Membrane surface	Middle biofilm	Mid - upper biofilm
Control (no RO22 bacteria)	 $x/l = 0.11$ ($x = 2.0 \mu\text{m}$)	 $x/l = 0.44$ ($x = 8.0 \mu\text{m}$)	 $x/l = 0.61$ ($x = 11.0 \mu\text{m}$)
Coag+ CMF feed (with RO22 and chloramin e)	 $x/l = 0.07$ ($x = 2.0 \mu\text{m}$)	 $x/l = 0.20$ ($x = 6.0 \mu\text{m}$)	 $x/l = 0.47$ ($x = 14 \mu\text{m}$)
Ozone+ coag+ CMF feed (with RO22)	 $x/l = 0.06$ ($x = 2.0 \mu\text{m}$)	 $x/l = 0.27$ ($x = 8.0 \mu\text{m}$)	 $x/l = 0.33$ ($x = 12.0 \mu\text{m}$)

753 **Figure 8:** Confocal images of RO membrane fouled by selected pre-treated wastewaters. The
754 distance from the membrane surface is represented by x , and shown as the ratio to the
755 estimated total fouling layer thickness l observed in the confocal imaging.

756

757 In considering the application of ozone prior to RO, in a previous pilot trial the lack of
758 biofouling observed was attributed to the use of BAC to digest organics prior to RO [18, 19].
759 However it may not be required to utilise BAC in all cases. In the 3000 hour pilot trial of RO
760 fed with MBR effluent (one train with added ozone, the other direct from MBR), no
761 operational issues due to biofouling were observed [15]. In fact, they concluded the train with
762 ozone had less biofouling as observed from protein analysis on the lead elements. Therefore,
763 while the biodegradability of organics increases as per the well-known effect of ozone and
764 UVH as shown in Table 5, the prior pilot trial results and our biofouling potential assessment
765 shown in Figure 7 and Figure 8 show that increased biodegradability of organics does not

766 necessarily lead to increased biofilm formation on RO membranes. On the contrary, both our
767 bioassay result (Figure 7), and the previously reported pilot trial, support the concept that
768 ozone reduces biofouling potential. This could be related to the reduced adhesion of organics
769 on the surface of the membrane that form the conditioning layer needed for a biofilm to
770 commence growth where recent studies have attributed lectin-like humics, which readily pass
771 MF membranes, as being a key compound in forming the conditioning layer leading to RO
772 membrane biofouling [23]. Ozone was shown earlier to generally reduce aromaticity and the
773 hydrophobic proportion of organics, and in particular to reduce the proportion of humic
774 substances in the organics. Removal of humics was even more enhanced by CMF after
775 oxidation (Figure 2) and less likely to deposit or diffuse into the RO membrane (Figure 4b).
776 Further, the oxidised foulants loaded on the RO membranes were more porous (Figure 5).
777 These may have played a key role in limiting the thickness of the active biofilm, despite the
778 organics being more easily assimilable. It appears that ozone (and potentially UVH) treatment
779 prior to RO is not likely to create additional biofouling operation issues. However, further
780 work is needed to confirm similar benefits on other wastewater matrices and process
781 conditions.

782

783 The results presented here are representative of a real system, but do not take into account
784 fouling by the actual biomass present in wastewaters, which vary with water source, for
785 example from sea water to wastewater, as well as between lead and tail elements [48]. Further
786 testing is recommended using long term pilot trials on the water to be treated, particularly at
787 recoveries typical of wastewater RO plants (70% to 90%). This would give a more precise
788 determination of actual biofouling risks and location along the membrane using indigenous
789 biological communities.

790

791 **Conclusions**

792 In the current study, pre-treatments of RO feed water with coagulation and oxidation processes
793 and filtration with ceramic membranes were proposed for application in wastewater recycling.
794 The main outcomes and recommendations from this work were as follows:

- 795 • More sustainable TMP at high CMF flux was achieved when oxidation (either ozone
796 or UVH) and coagulation was applied to the feed water from the WWTP;
- 797 • LC-OCD analysis of the various pre-treated waters used as RO feeds showed that CMF
798 can remove the biopolymers and coagulation removes humic substances. Oxidation by
799 ozone or UVH also removed biopolymers, but had a further effect on reducing humic
800 substances concentration. An unconfirmed increase in building blocks and LMW
801 organics was observed in the UVH+coagulation+CMF permeate;
- 802 • NDMA analysis of various pre-treated water samples showed an increase in NDMA
803 formation for all samples with chloramine addition, being similar except for UVH
804 which showed a lower relative increase. NDMA increase however was more significant
805 when ozone was used, which could influence the decision for its use (e.g. potable reuse)

806 in achieving high CMF fluxes. UVH on the other hand showed no NDMA increase,
807 where instead it reduced it to lower than the incoming feed water and may be more
808 favourable in such cases where NDMA must be controlled as it also enables high CMF
809 fluxes;

- 810 • The use of ozone or UVH increased the biodegradable organic fraction and growth of
811 RO22 bacteria in the wastewater, but crystal violet assay with RO22 bacteria showed
812 reduced formation of bacterial biofilm communities using ozone+coagulant+CMF
813 pre-treated waters compared to coagulant+CMF pre-treated. Accelerated RO
814 biofouling tests with RO22 bacteria confirmed the findings that despite having a
815 slightly thicker fouling layer, the active bacterial community in the ozone+coagulant+
816 CMF treated water was greatly limited in proximity to the membrane surface
817 compared to coagulant+CMF treated water. This was attributed to the reduction of
818 humic fraction concentrations and alteration of humic chemical properties (including
819 reduced aromaticity), and formation of more porous fouling layers on RO membranes
820 which are less adhesive and more easily removed by flowing water. The findings
821 provide evidence that biofouling due to biofilm formation on RO membranes may not
822 be an issue if upstream oxidation is applied to achieve high CMF fluxes; and
- 823 • Chloramine added to biofouling tests did not reduce cell activity in biofilms, but
824 appeared to assist in killing bacteria in the biofilm which extended more into the bulk
825 fluid;

826 Practical use of CMF as a pre-treatment for RO in advanced water treatment schemes is
827 recommended. However for achieving the high CMF fluxes needed for economical use of
828 ceramic membranes, options must consider the impact of oxidation where ozone leads to
829 potential for NDMA formation while UVH instead could require significant energy. Long term
830 pilot trials in specific contexts are recommended to further explore fouling and operating
831 requirements. As shown in our work with ozone, and as supported by bench and pilot tests by
832 other researchers, oxidation applied upstream of RO leads to minimised organic and biofouling
833 maintenance issues.

834

835 **Acknowledgements**

836 The authors acknowledge the financial support of City West Water, and the National Centre of
837 Excellence in Desalination Australia which is funded by the Australian Government through
838 the National Urban Water and Desalination Plan. The contributions to the project and work
839 presented in this paper by Dr David Halliwell from Water Research Australia and Chris
840 Arabatzoudis from City West Water are gratefully acknowledged.

841

842

843

844

845 **List of abbreviations**

846 BAC: biological activated carbon

847 BDOC: biodegradable dissolved organic carbon

848 BSA: bovine serum albumin

849 CMF: ceramic microfiltration

850 DOC: dissolved organic carbon

851 DBP: disinfection by-product

852 HIFI: hydraulic irreversible fouling index

853 LC-OCD: liquid size exclusion chromatography with organic carbon detection

854 LMW: low molecular weight

855 MF: microfiltration

856 MBR: membrane bioreactor

857 NDMA: N-nitrosodimethylamine

858 PACl: polyaluminium chloride

859 PS: polysulfone

860 PVDF: polyvinylidene fluoride

861 RO: reverse osmosis

862 SEM: scanning electron microscopy

863 SRP: salt reduction plant

864 SUVA: specific UV absorbance

865 TDS: total dissolved solids

866 TMP: transmembrane pressure

867 TOC: trace organic compounds

868 TSB: tryptone soy broth

869 UF: ultrafiltration

870 UMFI: unified membrane fouling index

871 UVH: ultraviolet/hydrogen peroxide

872 WWTP: wastewater treatment plant

873

874 **References**

875

876 [1] S.G. Lehman and L. Liu, *Application of ceramic membranes with pre-ozonation for treatment of*
877 *secondary wastewater effluent*. *Water Research*, 2009. **43**(7): p. 2020-2028.

878 [2] N. Dow, D. Murphy, J. Clement, and M. Duke, *Outcomes of the Australian Ozone/Ceramic*
879 *Membrane Trial on Secondary Effluent*. *AWA Water*, 2013. **40**(6): p. 45-51.

880 [3] N. Dow, J. Roehr, D. Murphy, L. Solomon, J. Mieog, J. Blackbeard, S. Gray, N. Milne, B. Zhu, A.
881 Gooding, J. Currie, G. Roeszler, J. Clement, and M. Duke, *Fouling mechanisms and reduced*
882 *chemical potential of ceramic membranes combined with ozone*. *Water Practice &*
883 *Technology*, 2015. **10**(4): p. 806-813.

884 [4] J. Haberkamp, A.S. Ruhl, M. Ernst, and M. Jekel, *Impact of coagulation and adsorption on DOC*
885 *fractions of secondary effluent and resulting fouling behaviour in ultrafiltration*. *Water*
886 *Research*, 2007. **41**(17): p. 3794-3802.

887 [5] W.S. Guo, S. Vigneswaran, and H.H. Ngo, *Effect of flocculation and/or adsorption as pretreatment*
888 *on the critical flux of crossflow microfiltration*. *Desalination*, 2005. **172**(1): p. 53-62.

889 [6] E. Vasyukova, R. Proft, J. Jousten, I. Slavik, and W. Uhl, *Removal of natural organic matter and*
890 *trihalomethane formation potential in a full-scale drinking water treatment plant*. *Water*
891 *Science and Technology: Water Supply*, 2013. **13**(4): p. 1099-1108.

892 [7] L. Fan, T. Nguyen, F.A. Roddick, and J.L. Harris, *Low-pressure membrane filtration of secondary*
893 *effluent in water reuse: Pre-treatment for fouling reduction*. *Journal of Membrane Science*,
894 2008. **320**(1-2): p. 135-142.

895 [8] O. González, A. Justo, J. Bacardit, E. Ferrero, J.J. Malfeito, and C. Sans, *Characterization and fate of*
896 *effluent organic matter treated with UV/H₂O₂ and ozonation*. *Chemical Engineering Journal*,
897 2013. **226**(0): p. 402-408.

898 [9] W. Yu, D. Zhang, and N.J.D. Graham, *Membrane fouling by extracellular polymeric substances after*
899 *ozone pre-treatment: Variation of nano-particles size*. *Water Research*, 2017. **120**: p. 146-155.

900 [10] S. Lee, K. Lee, W.M. Wan, and Y. Choi, *Comparison of membrane permeability and a fouling*
901 *mechanism by pre-ozonation followed by membrane filtration and residual ozone in*
902 *membrane cells*. *Desalination*, 2005. **178**(1): p. 287-294.

903 [11] M. Hashino, Y. Mori, Y. Fujii, N. Motoyama, N. Kadokawa, H. Hoshikawa, W. Nishijima, and M.
904 Okada, *Pilot plant evaluation of an ozone-microfiltration system for drinking water treatment*.
905 *Water Science and Technology*, 2000. **41**(10-11): p. 17-23.

906 [12] Y.G. Park, *Effect of ozonation for reducing membrane-fouling in the UF membrane*. *Desalination*,
907 2002. **147**(1): p. 43-48.

908 [13] X. Wang, L. Wang, Y. Liu, and W. Duan, *Ozonation pretreatment for ultrafiltration of the secondary*
909 *effluent*. *Journal of Membrane Science*, 2007. **287**(2): p. 187-191.

910 [14] B. Zhu, Y. Hu, S. Kennedy, N. Milne, G. Morris, W. Jin, S. Gray, and M. Duke, *Dual function filtration*
911 *and catalytic breakdown of organic pollutants in wastewater using ozonation with titania and*
912 *alumina membranes*. *Journal of Membrane Science*, 2011. **378**(1-2): p. 61-72.

913 [15] B.D. Stanford, A.N. Pisarenko, S.A. Snyder, and R.D. Holbrook, *Pilot-scale oxidative technologies*
914 *for reducing fouling potential in water reuse and drinking water membranes*. 2013, *Water*
915 *Reuse Association*.

916 [16] B.D. Stanford, A.N. Pisarenko, R.D. Holbrook, and S.A. Snyder, *Preozonation effects on the*
917 *reduction of Reverse Osmosis Membrane Fouling in Water Reuse*. *Ozone: Science &*
918 *Engineering*, 2011. **33**(5): p. 379-388.

- 919 [17] J. Zhang, K. Northcott, M. Duke, P. Scales, and S.R. Gray, *Influence of pre-treatment combinations*
920 *on RO membrane fouling*. *Desalination*, 2016. **393**: p. 120-126.
- 921 [18] J. Zhang, A. Knight, M. Duke, K. Northcott, M. Packer, P.J. Scales, and S.R. Gray, *A new integrated*
922 *potable reuse process for a small remote community in Antarctica*. *Process Safety and*
923 *Environmental Protection*, 2016. **104, Part A**: p. 196-208.
- 924 [19] J. Zhang, M. Duke, K. Northcott, M. Packer, M. Allinson, G. Allinson, K. Kadokami, J. Tan, S. Allard,
925 J.-P. Croué, A. Knight, P. Scales, and S. Gray, *Small scale direct Potable Reuse (DPR) Project for*
926 *a Remote Area*. *Water*, 2017. **9**(2): p. 94.
- 927 [20] B.S. Oh, H.Y. Jang, Y.J. Jung, and J.-W. Kang, *Microfiltration of MS2 bacteriophage: Effect of ozone*
928 *on membrane fouling*. *Journal of Membrane Science*, 2007. **306**(1-2): p. 244-252.
- 929 [21] S.T. Nguyen and F.A. Roddick, *Effects of ozonation and biological activated carbon filtration on*
930 *membrane fouling in ultrafiltration of an activated sludge effluent*. *Journal of Membrane*
931 *Science*, 2010. **363**(1-2): p. 271-277.
- 932 [22] K.I. Abdul Hamid, P. Sanciolo, S. Gray, M. Duke, and S. Muthukumaran, *Impact of ozonation and*
933 *biological activated carbon filtration on ceramic membrane fouling*. *Water Research*, 2017.
- 934 [23] H. Winters, T.H. Chong, A.G. Fane, W. Krantz, M. Rzechowicz, and N. Saeidi, *The involvement of*
935 *lectins and lectin-like humic substances in biofilm formation on RO membranes - is TEP*
936 *important?* *Desalination*, 2016. **399**: p. 61-68.
- 937 [24] W.A. Mitch, J.O. Sharp, R.R. Trussell, R.L. Valentine, L. Alvarez-Cohen, and D.L. Sedlak, *N-*
938 *Nitrosodimethylamine (NDMA) as a drinking water contaminant: a review*. *Environmental*
939 *Engineering Science*, 2004. **20**(5): p. 389-404.
- 940 [25] P. Andrzejewski, B. Kasprzyk-Hordern, and J. Nawrocki, *N-nitrosodimethylamine (NDMA)*
941 *formation during ozonation of dimethylamine-containing waters*. *Water Research*, 2008.
942 **42**(4-5): p. 863-870.
- 943 [26] P. Andrzejewski and J. Nawrocki, *N-nitrosodimethylamine (NDMA) as a product of potassium*
944 *permanganate reaction with aqueous solutions of dimethylamine (DMA)*. *Water Research*,
945 2009. **43**(5): p. 1219-1228.
- 946 [27] T. Bond, J. Huang, M.R. Templeton, and N. Graham, *Occurrence and control of nitrogenous*
947 *disinfection by-products in drinking water - A review*. *Water Research*, 2011. **45**(15): p. 4341-
948 4354.
- 949 [28] C.K. Schmidt and H.-J. Brauch, *N,N-Dimethylsulfamide as precursor for N-Nitrosodimethylamine*
950 *(NDMA) formation upon Ozonation and its Fate During Drinking Water Treatment*.
951 *Environmental Science & Technology*, 2008. **42**(17): p. 6340-6346.
- 952 [29] APHA, AWWA, and WEF, *Standard methods for the examination of water & wastewater*. 21st ed,
953 ed. A. Eaton, L.S. Clesceri, A.E. Greenberg, and E.W. Rice. 2005: American Water Works
954 Association (AWWA)
- 955 [30] H. Bader, V. Sturzenegger, and J. Hoigné, *Photometric method for the determination of low*
956 *concentrations of hydrogen peroxide by the peroxidase catalyzed oxidation of N,N-diethyl-p-*
957 *phenylenediamine (DPD)*. *Water Research*, 1988. **22**(9): p. 1109-1115.
- 958 [31] D.T. Myat, M. Mergen, O. Zhao, M.B. Stewart, J.D. Orbell, and S. Gray, *Characterisation of organic*
959 *matter in IX and PACl treated wastewater in relation to the fouling of a hydrophobic*
960 *polypropylene membrane*. *Water Research*, 2012. **46**(16): p. 5151-5164.
- 961 [32] H. Huang, T.A. Young, and J.G. Jacangelo, *Unified membrane fouling index for low Pressure*
962 *Membrane Filtration of Natural Waters: Principles and Methodology*. *Environmental Science*
963 *& Technology*, 2008. **42**(3): p. 714-720.
- 964 [33] A.H. Nguyen, J.E. Tobiasson, and K.J. Howe, *Fouling indices for low pressure hollow fiber membrane*
965 *performance assessment*. *Water Research*, 2011. **45**(8): p. 2627-2637.
- 966 [34] A.N. Pisarenko, D. Yan, S.A. Snyder, and B.D. Stanford, *Comparing oxidative organic oouling*
967 *Control in RO Membrane Applications*. *IDA Journal of Desalination and Water Reuse*, 2011.
968 **3**(2): p. 45-49.

- 969 [35] S.A. Huber, A. Balz, M. Abert, and W. Pronk, *Characterisation of aquatic humic and non-humic*
970 *matter with size-exclusion chromatography – organic carbon detection – organic nitrogen*
971 *detection (LC-OCD-OND)*. *Water Research*, 2011. **45**(2): p. 879-885.
- 972 [36] S.A. Huber and F.H. Frimmel, *A new method for the characterization of Organic Carbon in Aquatic*
973 *Systems*. *International Journal of Environmental Analytical Chemistry*, 1992. **49**(1-2): p. 49-57.
- 974 [37] J.C. Joret and Y. Levi, *Methode rapide d'evaluation du carbone eliminable des eaux par voie*
975 *biologique*. *Trib. Cebedeau*, 1986. **510**: p. 3-9.
- 976 [38] C. Volk, C. Renner, P. Roche, H. Paillard, and J.C. Joret, *Effects of ozone on the production Of*
977 *Biodegradable Dissolved Organic Carbon (BDOC) During Water Treatment*. *Ozone: Science &*
978 *Engineering*, 1993. **15**(5): p. 389-404.
- 979 [39] J.W.A. Charrois, M.W. Arend, K.L. Froese, and S.E. Hrudey, *Detecting N-nitrosamines in drinking*
980 *water at Nanogram per Liter Levels Using Ammonia Positive Chemical Ionization*.
981 *Environmental Science & Technology*, 2004. **38**(18): p. 4835-4841.
- 982 [40] G.A. O'Toole, *Microtiter dish biofilm formation assay*. *Journal of Visualized Experiments : JoVE*,
983 2011(47): p. 2437.
- 984 [41] V. Nagaraj, L. Skillman, D. Li, A. Foreman, Z. Xie, and G. Ho, *Characterisation of extracellular*
985 *polysaccharides from bacteria isolated from a full-scale desalination plant*. *Desalination*, 2017.
986 **418**: p. 9-18.
- 987 [42] M.R. Jekel, *Flocculation effects of ozone*. *Ozone: Science & Engineering*, 1994. **16**(1): p. 55-66.
- 988 [43] B. Domenjoud, N. Cortés-Francisco, R. Guastalli Andrea, J. Caixach, S. Esplugas, and S. Baig,
989 *Ozonation of municipal secondary ffluent; Removal of Hazardous Micropollutants and Related*
990 *Changes of Organic Matter Composition*, in *Journal of Advanced Oxidation Technologies*. 2011.
991 p. 138.
- 992 [44] R.H.S. Jansen, A. Zwijnenburg, W.G.J. van der Meer, and M. Wessling, *Outside-in trimming of*
993 *humic Substances During Ozonation in a Membrane Contactor*. *Environmental Science &*
994 *Technology*, 2006. **40**(20): p. 6460-6465.
- 995 [45] X. Liao, C. Chen, B. Yuan, J. Wang, and X. Zhang, *Control of nitrosamines, THMs, and HAAs in*
996 *heavily impacted Water With O3-BAC*. *Journal - American Water Works Association*, 2017.
997 **109**(6): p. E215-E225.
- 998 [46] D. Gerrity, A.N. Pisarenko, E. Marti, R.A. Trenholm, F. Gerringer, J. Reungoat, and E. Dickenson,
999 *Nitrosamines in pilot-scale and full-scale wastewater treatment plants with ozonation*. *Water*
1000 *Research*, 2015. **72**: p. 251-261.
- 1001 [47] S.W. Krasner, W.A. Mitch, D.L. McCurry, D. Hanigan, and P. Westerhoff, *Formation, precursors,*
1002 *control, and occurrence of nitrosamines in drinking water: A review*. *Water Research*, 2013.
1003 **47**(13): p. 4433-4450.
- 1004 [48] M.T. Khan, M. Busch, V.G. Molina, A.-H. Emwas, C. Aubry, and J.-P. Croue, *How different is the*
1005 *composition of the fouling layer of wastewater reuse and seawater desalination RO*
1006 *membranes?* *Water Research*, 2014. **59**: p. 271-282.
- 1007 [49] J.S. Vrouwenvelder and D. van der Kooij, *Diagnosis, prediction and prevention of biofouling of NF*
1008 *and RO membranes*. *Desalination*, 2001. **139**(1): p. 65-71.

1009